Natural Hazards
https://doi.org/10.1007/s11069-024-06708-9

ORIGINAL PAPER

Temporal variability of sinkhole hazard illustrated in the western shore of the Dead Sea

Jorge Sevil[1] · **Francisco Gutiérrez**[1]

Received: 15 March 2023 / Accepted: 21 May 2024

Abstract
The growing economic and societal damage caused by sinkhole activity worldwide requires the development of scientifically sound sinkhole hazard assessment approaches. Currently, there is a striking paucity of quantitative sinkhole hazard studies largely related to the incompleteness of sinkhole inventories and the lack of chronological data. Moreover, the probability of occurrence of sinkholes (i.e., sinkhole hazard) is commonly considered as a steady variable, a concept that may lead to significant hazard over- or under-estimates. The extraordinarily high frequency of sinkhole occurrence of the studied sector of the western shore of the Dead Sea has allowed us to explore for the first time the potential temporal variability of sinkhole hazard parameters. Here, we produced six multi-temporal sinkhole inventories with morphometric data between 2005 and 2021 using remote-sensed imagery. The frequency-size relationships generated for successive time intervals with a total of 667 new sinkholes reveal substantial temporal changes in the sinkhole hazard components (i.e., frequency and size). Moreover, the work illustrates that spatial redundancy (sinkholes nested within or intersecting pre-existing ones) can lead to significant hazard overestimates if not considered, especially in areas with high sinkhole density and clustering. This work discusses the limitations of some widely used methods and concepts for sinkhole hazard assessment and illustrates the advantages of detailed multi-temporal mapping for assessing frequency-size relationships and their temporal trends.

Keywords Multi-temporal mapping · Spatial redundancy · Frequency-size relationships · Effective hazard · Temporal trend

1 Introduction

Active sinkholes cause risk situations worldwide with important economic and societal implications. Gutiérrez (2016) listed some of the most damaging sinkhole events reported in the literature, occurred in countries such as Spain, South Africa, Kuwait, United States, China, or Russia. As illustrated by these examples, sinkholes can cause economic losses amounting millions of euros, the evacuation of population, the demolition of residential

✉ Jorge Sevil
jorgesevil@unizar.es

[1] Departamento de Ciencias de la Tierra, Universidad de Zaragoza, Zaragoza, Spain

and industrial buildings, service interruptions in major transportation infrastructure, and even fatalities. Population and economic growth have resulted in an increase of the vulnerable elements exposed to natural damaging processes. Moreover, very often sinkhole activity is triggered or accelerated by human activities that modify karst environments (Cooper 2002; Beck 2012; Song et al. 2012; Parise et al. 2015; Parise 2019; De Waele and Gutierrez 2022). Therefore, there is an increasing need for developing sinkhole hazard assessments, but the underlying concepts and methodologies have been scarcely studied, in contrast to other ground-instability hazardous processes such as landslides.

Waltham et al. (2005) defined sinkhole hazard as the probability of a sinkhole of a particular magnitude occurring in a given area and within a specific period of time. That is, the spatiotemporal probability of occurrence of an event with a specific magnitude (e.g., Cruden and Fell 2018). Nevertheless, there are multiple approaches for conducting hazard assessments. The vast majority consider two elements: (1) the size of the event; and (2) its frequency (or probability of occurrence), separately or in combination. For example, there are methods for hazard estimation that take into account the frequency of occurrence of events regardless of their size (e.g., Remondo et al. 2005), some consider the annual increment of the area affected by the process (e.g., Hufschmidt and Crozier 2008), others estimate an average size for the process and apply theoretical probability functions to forecast its size distribution (e.g., Tolmachev and Leonenko 2011), or evaluate the frequency-size relationships (e.g., Galve et al. 2011; Taheri et al. 2015). In this regard, frequency-size relationships are commonly applied in hazard studies to model spatiotemporal distribution functions that describe the empirical data and serve to establish future projections for risk management (Malamud 2004; Corral and González 2019; Bernatek-Jakiel et al. 2019). They were firstly applied by Gutenberg and Ritcher (1954) to describe the empirical relation between the magnitude of an earthquake and its cumulative frequency. Afterwards, they have continued to be used to further investigate earthquakes (e.g., Pacheco et al. 1992; Coppersmith et al. 2009; Bayrak et al. 2015) and other hazardous geological processes such as landslides (e.g., Dai and Lee 2001; Guzzetti et al. 2002; Malamud et al. 2004; Remondo et al. 2005; Casas et al. 2016; Corominas et al. 2018), floods (e.g., Machado et al. 2015; Cloete et al. 2018; Chiverrell et al. 2019), piping collapses (Bernatek-Jakiel et al. 2019), and sinkholes (Galve et al. 2009, 2011; Tolmachev and Leonenko 2011; Taheri et al. 2015; Gutiérrez and Lizaga 2016).

Despite the growing amount of research addressing different aspects of sinkholes (see review in Gutiérrez et al. 2014), there is a notable lack of quantitative hazard assessments. This scarcity is generally caused by: (1) the incompleteness of sinkhole inventories; (2) the common low rate of sinkhole occurrence and thus the limited chronological data; and (3) the lack of data on the sinkhole size at the time of occurrence. In the Ebro Valley, Spain, Galve et al., (2009; 2011) presented quantitative sinkhole hazard models including frequency-size relationships, but based on size data with limited accuracy. In Hamedan, Iran, Taheri et al. (2015) produced frequency-size relationships, but based on a limited number of events.

Sinkhole hazard analyses are often based on incomplete sinkhole inventories providing minimum estimates (Gutiérrez 2016). Moreover, in most cases it is implicitly considered that sinkhole hazard remains constant over time, which is an uncertain assumption that may lead to significant hazard under- or over-estimates. Cruden and Hu (1993) introduced for the first time a non-steady statistical approach to model the temporal distribution of rock slides, called exhaustion model, whereby, given a limited number of potential sliding sites, the probability of occurrence would decrease after slope movement and landform stabilization. Subsequent works on hazard assessment evaluated the potential variability

of frequency and size of hazardous processes related to the geomorphic setting (e.g., Hufschmidt and Crozier 2008), geological constraints (e.g., Corominas et al. 2018), or external factors such as urban development, land-use variation, or climate change (e.g., van Westen et al. 2006; Bonachea et al. 2009; Crozier 2010; Kundzewicz et al. 2017; Hounkpè et al. 2019; Bates et al. 2021). The changes in hazardous systems have crucial consequences on the accuracy and reliability of hazard and risk predictions and could reduce the effectiveness of mitigation measures.

To our knowledge, sinkhole hazard assessments published in the literature have never evaluated the temporal variability of frequency-size relationships. Nevertheless, the highly active salt karst of the Dead Sea, and the technical possibility of obtaining data on sinkhole occurrence with high temporal and spatial resolution, offer an exceptional opportunity to comprehensively assess hazard and its temporal evolution. Here, thousands of human-induced sinkholes have formed since 1980s in parallel with a persistent lake level decline mainly because of the use of water from its catchment and the lake itself (Abelson et al. 2006). The extraordinary high rate of sinkhole occurrence allows assessing, within a relatively short investigation period, sinkhole hazard from a dynamic perspective. The analysis, based on complete sinkhole inventories including chronological and size data of each sinkholes, illustrates the temporal variability of sinkhole hazard. Despite sinkholes occurring on the western and eastern coast of the Dead Sea have been extensively studied in recent years (Frumkin and Raz 2001; Baer et al. 2002, 2018; Abelson et al. 2006; Closson and Karaki 2009; Ezersky et al. 2009; Filin et al. 2011; Avni et al. 2016; Yechieli et al. 2016; Al-Halbouni et al. 2017, 2019, 2021; Yizhaq et al. 2017; Nof et al. 2019; Watson et al. 2019; Arav et al. 2020; Ezersky and Frumkin 2020, 2021; Sevil and Gutiérrez 2023) and constitute a highly damaging process, no quantitative hazard analyses have been conducted so far.

2 Geological setting

The Dead Sea is a hyper-saline endorheic lake located at the lowest elevation on Earth (~437 m below sea level in 2021 according to the geodetic data gathered by Sevil and Gutiérrez 2023). It lies at the bottom of the Dead Sea pull-apart basin, associated with the left-stepping Arava and Jericho strike-slip faults. These NNE-trending structures occur in the southern sector of the left-lateral Dead Sea transform fault system, between the Arabian plate and the Sinai sub-plate (Garfunkel and Ben-Avraham 1996) (Fig. 1a). The study area, covering 2 km^2, is located on the western coast of the Dead Sea, in the piedmont of the Western Boundary Fault escarpment, extending between the Nahal Hazezon alluvial fan and 100 m north of the Ein Kedem North thermal spring. The Western Boundary Fault juxtaposes Holocene Ze'elim lake deposits in the downthrown block against the Late Pleistocene Samra and Lisan lacustrine formations, deposited in much larger paleolakes. The underlying bedrock consists of carbonate units of the Judean Mountains (Mor and Burg 2000; Neugebauer et al. 2014; Coianiz et al. 2019, 2020) (Fig. 1b). From west to east, the area comprises three morpho-sedimentary environments: (1) a strip of steep slopes underlain by colluvial deposits shed from the fault escarpment; (2) alluvial fans consisting of slightly cemented gravels; and (3) a mudflat on soft, laminated lake deposits exposed by the human-induced decline of the lake level (Fig. 1c–d).

The studied sinkholes mostly occur in the mudflat, and to a much lesser extent in the southern sector of the Nahal Hazezon alluvial fan. At the boundary between these two

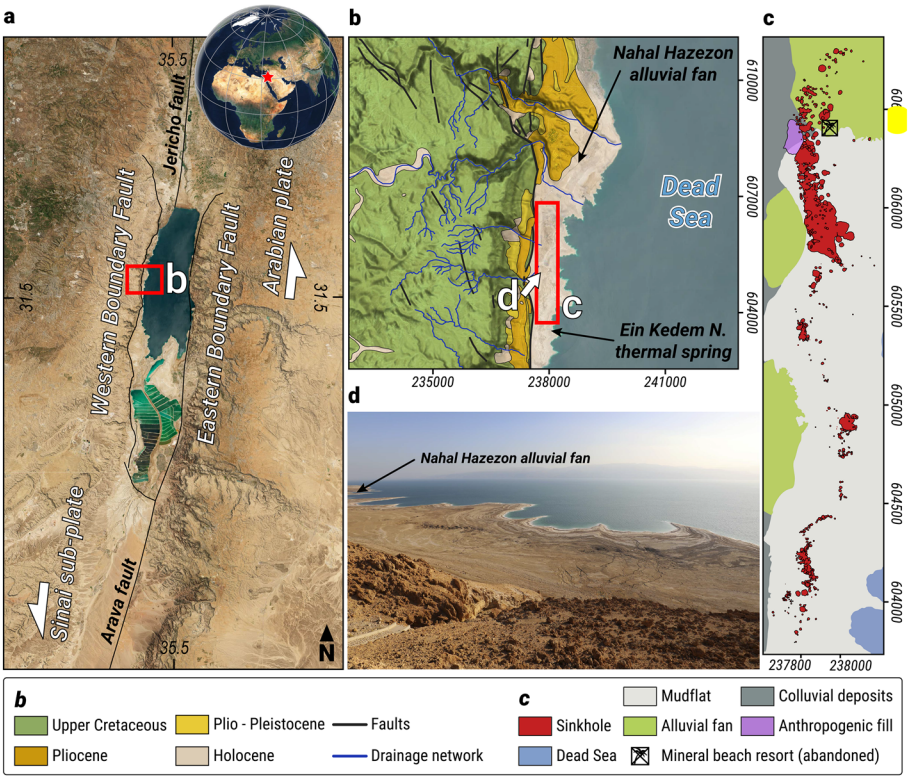

Fig. 1 Geological setting of the study area. a. Satellite image of the Dead Sea located within the pull-apart basin developed between the Arabian plate and the Sinai sub-plate. b. Geological sketch including the studied sector in the western coast of the Dead Sea, south of the Nahal Hazezon alluvial fan (modified from Mor and Burg 2000). c. Geomorphological map of the study area indicating the main morpho-sedimentary units and the sinkholes mapped in 2021 (modified from Sevil and Gutiérrez 2023). Coordinate system in b and c EPSG:2039. d. Image of the study area taken from the southwestern escarpment

geomorphic units sinkhole activity caused the destruction and abandonment of the Mineral Beach touristic resort (Fig. 1c). Here, there is thermal deep groundwater rising at 30 °C and unsaturated with respect to halite, with a salinity of ca. 120 g/L (halite solubility 356 g/L, per liter of solvent) (Abelson et al. 2006; Yechieli et al. 2006). In the analyzed area, the Ze'elim Fm. consists of interdigitated gravelly alluvial fan and lacustrine muds, and a basal porous and poorly lithified (i.e., eogenic) halite unit 13–18 m thick at around 20–30 m depth that pinches out to the west. Borehole data indicate a significant lakeward elevation drop of the top and bottom of the salt in short distances (10 m in 200 m distance) (Frumkin et al. 2011; Ezersky and Frumkin 2013), suggesting that the unit is vertically offset by a concealed down-to-the-east fault, as supported by seismic reflection profiles (Abelson et al. 2003) and the linear distribution of sinkholes. The displacement of the brackish-saline groundwater interface induced by the lake-level drop, and the accompanying dissolution of the salt unit, has resulted in the generation of the more than 6000 sinkholes since 1980 on the western coast of the Dead Sea (Abelson et al. 2006; Yechieli et al. 2006), damaging transportation infrastructure and tourist resorts, and compromising human safety (e.g., Frumkin et al. 2011; Abou Karaki et al. 2016; Salameh et al. 2019; Vey et al. 2021). Three

main compatible models have been proposed to explain the dissolution of the salt unit: (1) deep groundwater from bedrock aquifers rising along concealed faults (hypogene karst) (Abelson et al. 2003; Closson 2005; Shalev et al. 2006; Frumkin et al. 2011; Closson et al. 2013; Charrach 2019); (2) shallow groundwater from the marginal alluvial fan gravels that dissolves the salt unit along its edge (e.g., Ezersky et al. 2009; Frumkin et al. 2011); and (3) surface water that percolates via sinkholes acting as swallow holes during flash floods (Avni et al. 2016; Arav et al. 2020).

3 Methodology

In order to analyze the frequency-size relationships of sinkholes (i.e., sinkhole hazard) and their temporal variability, we produced six multi-temporal sinkhole maps with a time lapse of three years, ranging from 2.8 to 3.9 years and spanning the period 2005–2021. Sinkhole mapping was conducted using the following remote-sensed imagery: (1) aerial photographs from 2005 to 2011 (100–66 cm/pix; Geological Survey of Israel); (2) satellite images from 2015 (25 cm/pix; Geological Survey of Israel); and (3) high-resolution orthomosaics (4 cm/pix) and digital surface models (14–17 cm/pix) that we produced by Structure from Motion (SfM) Photogrammetry with drone images taken by Terrascan-Labs LTD during two fieldwork campaigns conducted in 2018 and 2021. Despite the lower resolution of the imagery covering the older periods (2005–2011), the higher quality of the subsequent data, together with the barren and relatively flat nature of the area (Fig. 1d), allowed the precise mapping of the sinkhole edges in a GIS environment, producing detailed and complete time-lapse sinkhole inventories (Sevil and Gutiérrez 2023). The multi-temporal sinkhole maps capture four important processes involved in the evolution of the sinkhole field: (1) new sinkhole occurrence; (2) sinkhole reactivation; (3) sinkhole expansion by mass wasting processes; and (4) sinkhole coalescence related to the lateral growth of adjoining sinkholes or the formation of new sinkholes intersecting pre-existing ones, to form compound sinkholes.

In contrast to the previous analysis on the morphometric and spatiotemporal evolution of the sinkholes (Sevil and Gutiérrez 2023), in this hazard-oriented work we mainly focus our analysis on the new single sinkholes occurred over each time interval (2005–2008, 2008–2011, 2011–2015, 2015–2018, 2018–2021). The new sinkholes were classified into non-redundant and redundant, depending on whether they occurred in areas previously unaffected by sinkholes, or if they were nested into or intersecting pre-existing ones (Fig. 2). The underlying concept behind the differentiation of redundant sinkholes is that they may not involve any increase in the area affected by subsidence. The mapped sinkholes can be classified as cover collapse sinkholes and cover collapse and sagging sinkholes. Since the collapse mechanism is the dominant process in all the mapped sinkholes, they were analysed jointly. Two morphometric parameters were automatically extracted for each new sinkhole: length (distance between antipodal points) and area. These values can be considered as a good approximation to the size of the sinkholes at the time of occurrence given the temporal resolution of the data, and consequently adequate for conducting hazard assessments. The data was processed with the assistance of R (R Core Team 2022) and the packages tidyverse (Wickham et al. 2019) and sf (Pebesma 2018).

The frequency-size relationships of the new sinkholes occurred in different time intervals were explored considering their length. Very similar results would be obtained with the area, given the high circularity of the sinkholes, with a mean circularity ratio of 0.93

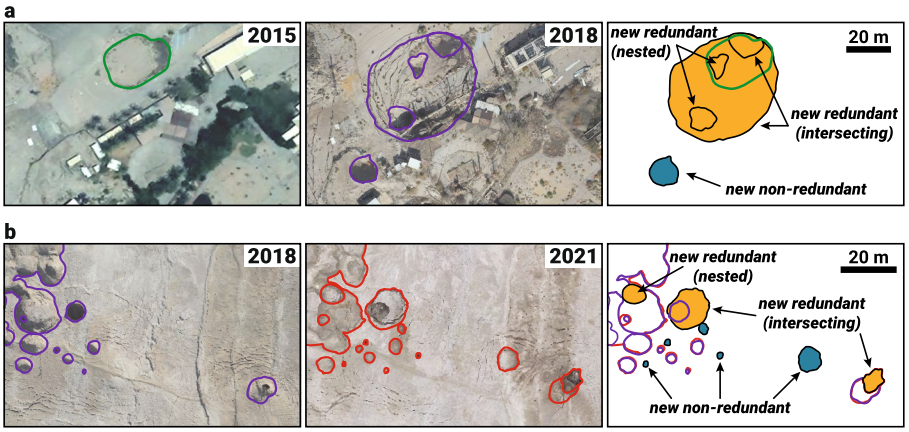

Fig. 2 Examples illustrating the difference between new non-redundant sinkholes and new redundant sinkholes, occurring in areas previously unaffected or affected by sinkholes, respectively. The orthoimages show changes occurred over the time intervals 2015–2018 (**a**), and 2018–2021 (**b**). Note that new sinkholes can be fully redundant or partially redundant depending on whether they are nested within pre-existing sinkholes or intersect previous sinkholes, respectively. The former does not involve any increase in the area affected by sinkholes

(ratio between sinkhole area and area of a circle with the same perimeter). We plotted sinkhole length (L) in logarithmic scale against the number of sinkholes equal or larger than a given size by unit area and time (i.e., cumulative spatiotemporal frequency; number of sinkholes $\geq$ L per km^2 and per year).

4 Results

The sinkholes mapped in the study area are confined within a narrow N–S trending strip including alignments and tightly packed clusters (Sevil and Gutiérrez 2023). Sinkhole coalescence played an important role in the evolution of the sinkhole field because of three main factors: (1) highly clustered distribution; (2) high rate of new sinkhole occurrence; and (3) rapid expansion of the steep-sided sinkholes by mass wasting. Overall, new sinkholes expanded the sinkhole belt towards the lake and progressively filled the space between the sinkhole clusters (Fig. 3). Sinkholes at the time of formation had a mean length of 5.6 m (0.6 – 35.0 m range) and an average area of 30.6 m^2 (0.2 – 658.5 m^2 range). The number of new sinkholes (197, 119, 151, 128, and 72) and the spatiotemporal frequency of sinkhole occurrence, expressed as number of sinkholes per km^2 and year (24.9, 21.3, 19.3, 19.6, 12.0) shows a general decrease throughout the analyzed time intervals (2005–2008, 2008–2011, 2011–2015, 2015–2018, 2018–2021) (Fig. 4a). The frequency of new sinkholes in the interval 2018–2021 was around half of that in 2005–2008 (24.9 vs. 12.0 sinkholes/km^2 yr).

As expected for a sinkhole field with high clustering and areal density, the proportion of redundant sinkholes increased substantially through time. The percentage of redundant sinkholes nested in or intersecting pre-existing ones escalated from 3% in 2005–2008 to 53% in 2018–2021. For the same time intervals, the spatiotemporal frequency of new redundant sinkholes increased from 0.6 to 6.4 sinkholes km^{-2} yr^{-1} (Fig. 4a). The

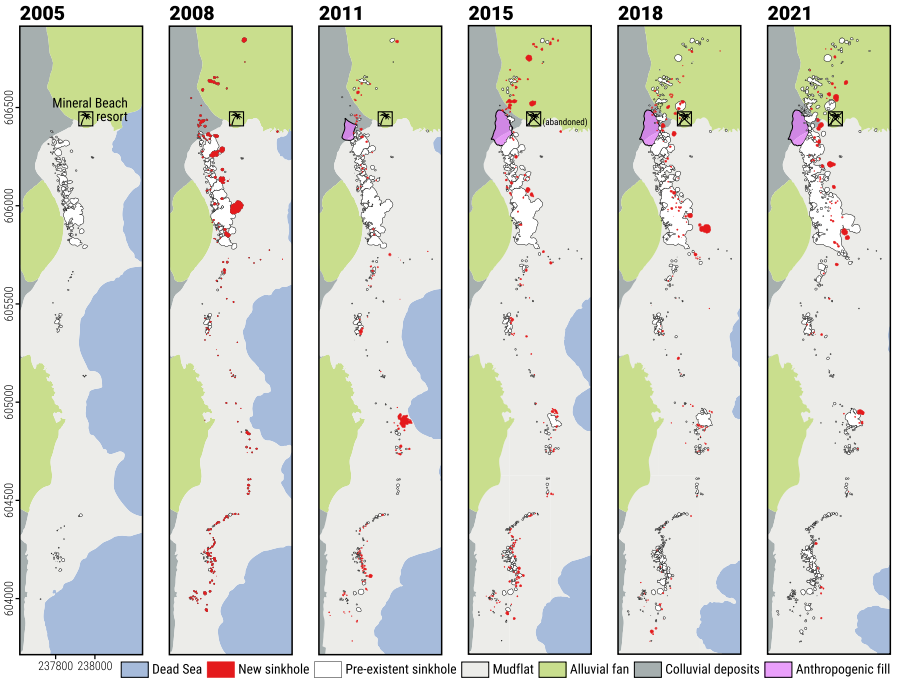

Fig. 3 Evolution of the spatiotemporal distribution of sinkholes between 2005 and 2021 (modified from Sevil and Gutiérrez 2023). The maps of the study area differentiate new sinkholes and pre-existing ones. The sequence records the lake-level decline and the consequent expansion of the mudflat. The maps also indicate the location of the Mineral Beach touristic resort that was abandoned in 2015 because of sinkhole damage and the anthropogenic fill dumped between 2008 and 2011 to mitigate sinkhole risk. Coordinate system EPSG:2039

progressive rise in spatial redundancy reflects the reduction in the sinkhole-free area and the densification of the sinkhole field (i.e., competition for space; De Waele and Gutierrez 2022).

Despite the decrease in sinkhole frequency and the growing spatial redundancy, the area affected by single non-redundant sinkholes showed a steady increase, indicating relatively constant areal increments (Fig. 4b). This apparent inconsistency is explained by the general increase in the size of the new sinkholes (Fig. 4c). The average length of the new non-redundant single sinkholes increased from 5.0 in 2005–2008, to 8.4 m in 2018–2021. Overall, the study area has been affected by progressively lower numbers of new sinkholes with higher spatial redundancy, but because of their larger dimensions, the sinkhole-affected area has increased steadily.

Figure 5 shows cumulative frequency-size relationships of all new single sinkholes and non-redundant new single sinkholes for different time intervals (i.e., hazard curves). The cumulative spatiotemporal frequency is expressed as the number of new sinkholes equal or larger than L (length) per km^2 and per year. The comparison between the "all new" and "only non-redundant" curves allows assessing the deviation between hazard curves generated considering and obviating spatial redundancy. The empirical data can be satisfactorily modelled over most of the size distribution by logarithmic functions with high goodness of fit (R^2_{adj} 0.94–0.98). Interestingly, most large new sinkholes are non-redundant (Fig. 5a).

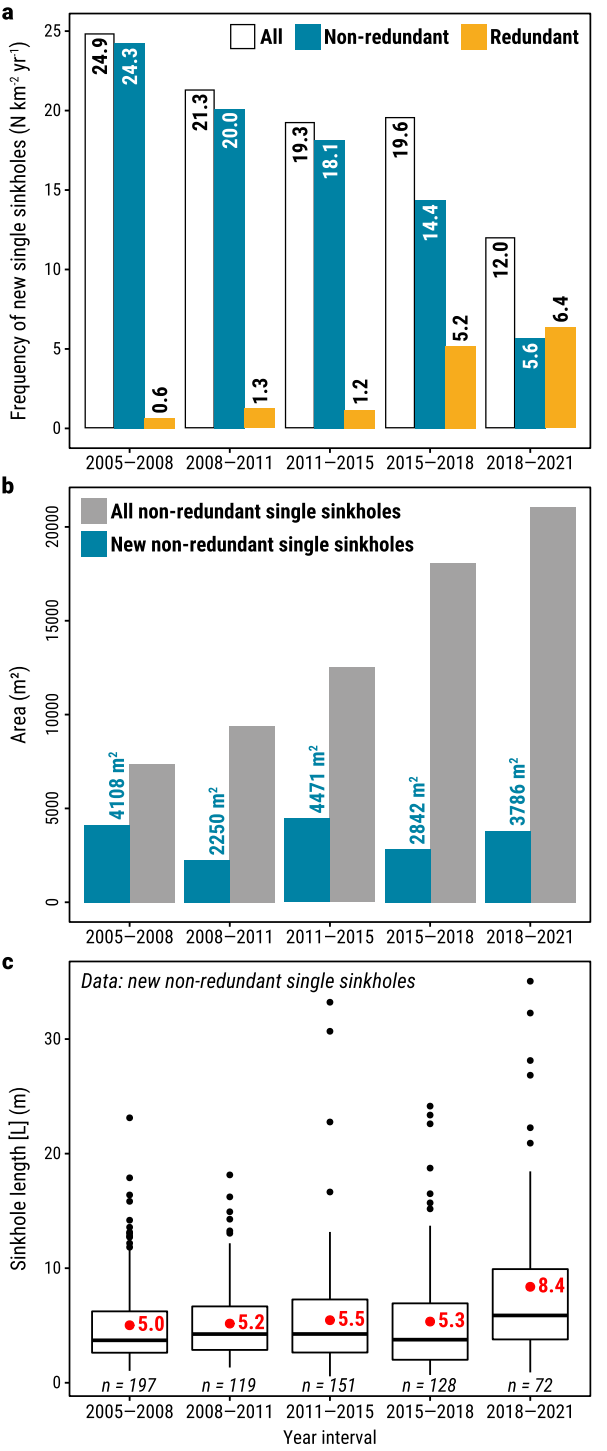

Fig. 4 Evolution of the new single sinkholes mapped in the study area over each year interval from 2005 to 2021. a. Spatiotemporal frequency differentiating redundant and non-redundant sinkholes. b. Comparison between the cumulative area of new and all non-redundant single sinkholes. c. Lengths of all the new non-redundant single sinkholes mapped in each year interval. The boxplots include in red the mean length

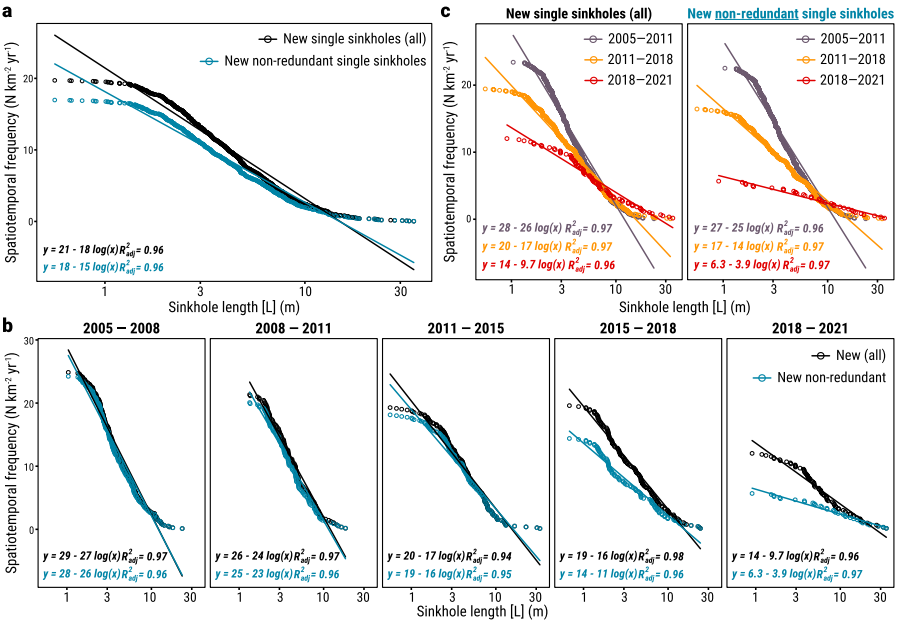

Fig. 5 Cumulative frequency-size relationships of all new single sinkholes and new non-redundant single ones for different time intervals. The plots include the logarithmic functions that better fit the empirical distributions (function and adjusted R^2 ($R.^2_{adj}$)). a. Frequency-size relationships of new single sinkholes at any time from 2005 to 2021. b. Frequency-size relationships at the time of occurrence. c. Frequency-size relationships for three successive time periods (2005–2011, 2011–2018, 2018–2021)

This is explained by the fact that new large sinkholes essentially occur on the east side of the sinkhole belt, away from pre-existing sinkholes, as indicated by the multi-temporal mapping (Fig. 3). The frequency-size relationships of new sinkholes formed during the different time intervals show a substantial deviation between the "all new" and "only non-redundant" curves from 2015 onwards, indicating the time at which spatial redundancy starts to have a significant impact in the decrease of the effective hazard (i.e., subsidence in previously unaffected areas). The frequency-size relationships representing new sinkholes for three successive time periods (2005–2011, 2011–2018, 2018–2021) show a progressive slope decline and an intersection point at ca. 10 m length (Fig. 5c). This indicates a significant decrease in the frequency of sinkholes smaller than 10 m and an increase in the frequency of larger sinkholes.

5 Discussion

The production of complete multi-temporal cartographic sinkhole inventories with morphometric data in a salt karst area characterized by extraordinarily high frequency of sinkhole occurrence and high clustering has allowed us to explore: (1) the potential impact of the commonly disregarded spatial redundancy on hazard assessments; (2) the advantages and disadvantages of different hazard assessment approaches; and (3) the temporal variability of sinkhole hazard.

Regarding spatial redundancy, the underlying concept is that redundant sinkholes do not necessarily involve an increase in the area affected by sinkholes, and consequently their consideration may lead to hazard overestimates (e.g., new sinkholes nested in pre-existing ones). In the analyzed zone, the available sinkhole-free area is rapidly exhausted because of the high rate of sinkhole occurrence, tight sinkhole clustering, and rapid expansion of the sinkholes by mass wasting. This explains the important morphogenetic role played by sinkhole coalescence and the high competition for space leading to significant spatial redundancy. Moreover, the rapid areal growth of the sinkholes has a significant impact on the establishment of set-back distances and the delineation of standoff zones. Sinkhole hazard can be markedly different in theoretical sinkhole fields with the same frequency of sinkhole occurrence, but with different clustering and sinkhole density. Spatial redundancy is higher in sinkhole fields with tight clustering, and it increases through time in specific fields as the areal density of sinkholes increases. In our particular case, spatial redundancy shows a substantial increase from 2015 onwards. The proportion of new redundant sinkholes in the interval 2005–2008 was 2%, whereas in the intervals 2015–2018 and 2018–2021 raised to 27% and 53%, respectively (Fig. 4a). Consistently, the frequency-size relationships (i.e., hazard curves) for "all new" and "only non-redundant" sinkholes start to show a significant deviation from 2015 (Fig. 5b). Hazard curves generated with all the new sinkholes suggest a significantly higher subsidence hazard than the more reasonable "effective hazard" curves obviating the new redundant sinkholes (Fig. 5).

Sinkhole hazard can be assessed using various parameters and approaches. A widely accepted parameter is the spatiotemporal frequency of sinkhole occurrence regardless of sinkhole size, expressed as number of sinkholes per unit area and time. Abelson et al. (2006) reported an acceleration trend in the occurrence rate of sinkholes in the Dead Sea from the 1980s to 2002. In our study area, we have observed a substantial decrease in the frequency of sinkhole occurrence dropping from 24.9 to 12.0 sinkholes km^{-2} yr^{-1}, suggestive of a significant hazard decrease. The sinkhole frequency decline is even more important when considering only non-redundant sinkholes for the same intervals (from 24.2 to 5.7). Sinkhole hazard can also be assessed computing the area affected by new sinkholes per unit time, implicitly integrating sinkhole frequency and size. In our study area, the areal increments remain relatively constant through time, suggesting a relatively unchanged hazard level. The apparent contradiction with the hazard assessment based on the number of new sinkholes is related to the occurrence of progressively larger sinkholes (Fig. 4).

Sinkhole hazard can be appraised more comprehensively generating empirical frequency-size relationships. The hazard curves generated for different time intervals (Fig. 5c) show a progressive flattening, apparently suggesting an overall declining hazard trend. The distribution of the curves indicates a substantial decrease in the frequency of small sinkholes and a slight increase in the frequency of large sinkholes. For instance, for the intervals 2005–2011 and 2018–2021, the frequency of new non-redundant sinkholes ≥ 2 m long dropped from 20.6 to 4.8 sinkholes per km^2 and year, whereas that of new non-redundant sinkholes ≥ 20 m long increased from 0.1 to 0.8 sinkholes per km^2 and year. The latter frequency increase is comparatively small but has a critical contribution to the hazard because of three main reasons. First, the area of a circular sinkhole 20 m long is equivalent to the area of 100 circular sinkholes 2 m long. Second, the capability of collapse sinkholes to cause damage (i.e., severity) largely depends on the sinkhole size at the time of occurrence. Third, the maximum observed sinkhole size is frequently used as the design parameter for sinkhole-resistant structures. This value has increased for the cover collapse sinkholes of the study area from 23 to 35 m between 2005–2011 and 2018–2021.

An interesting spatiotemporal pattern observed in the study area is the occurrence of larger sinkholes on the western sector of the subsidence belt, at some distance from the pre-existing sinkholes (non-redundant). A probable explanation is that dissolution is migrating toward the downthrown side of the concealed fault inferred by seismic data that has controlled the sinkhole strip (Abelson et al. 2006), and that has offset vertically the salt layer, as supported by borehole data (Ezersky and Frumkin 2013). This interpretation whereby dissolution is advancing toward areas with thicker overburden is compatible with the decrease in sinkhole frequency and the size increase of the sinkholes, although it remains as an untested hypothesis due to lack of sufficient subsurface data (e.g., boreholes).

6 Conclusions

In this research paper we show that sinkhole hazard can significantly change over time. The non-steadiness of the frequency-size relationships has important consequences inasmuch as it restricts the reliability and temporal validity of the hazard assessments.

In the study area of the western shore of the Dead Sea, the frequency-size relationships have displayed contrasting temporal changes in different sinkhole hazard components. Regarding the frequency of generation of new sinkholes, regardless of their size, sinkhole hazard showed a decreasing pattern. By contrast, the increment of the area affected by new non-redundant sinkholes displayed little variation suggesting rather constant hazard levels. However, the mean and maximum size of new sinkholes increased in time together with their relative frequency revealing a hazard and severity rise.

Moreover, the spatial redundancy of sinkholes, controlled by clustering and coalescence related to sinkhole interception or post-collapse expansion by mass wasting processes, can change the susceptibility status of the system and reduce the effectiveness of the damaging process. This characteristic is commonly disregarded on sinkhole hazard assessments and may cause their overestimation.

The presented results are applicable to other sinkhole-prone areas worldwide and illustrate that comprehensive hazard assessments require the construction of complete cartographic sinkhole inventories with chronological and morphometric data. Moreover, it is advisable to explore the temporal variability of frequency-size relationships to produce more reliable hazard estimates and better understand the controlling factors.

Acknowledgements The authors would like to thank the Geological Survey of Israel, and in particular Dr. Yoseph Yechieli, Dr. Gideon Baer and Dr. Meir Abelson for their valuable help and for providing aerial photographs and satellite data.

Author contributions Conceptualization: Francisco Gutiérrez and Jorge Sevil; Methodology and Data Curation: Jorge Sevil; Formal analysis and investigation: Jorge Sevil; Visualization: Jorge Sevil; Writing—original draft preparation: Jorge Sevil; Writing—review and editing: Francisco Gutiérrez; Funding acquisition: Francisco Gutiérrez; Supervision: Francisco Gutiérrez; Project administration: Francisco Gutiérrez.

Funding Open Access funding provided thanks to the CRUE-CSIC agreement with Springer Nature. This work has been supported by projects CGL2017-85045-P and PID2021_123189NB-I00 (Ministerio de Ciencia, Innovación y Universidades, Gobierno de España). Jorge Sevil has a pre-doctoral contract (PRE2018-084240) co-financed by the Spanish Government and the European Social Fund (ESF).

Data availability Data will be made available on request.

Declarations

Conflict of interest The authors have no competing interests to declare that are relevant to the content of this article.

References

Abelson M, Yechieli Y, Crouvi O, Baer G, Wachs D, Bein A, Shtivelman V (2006) Evolution of the Dead Sea sinkholes. GSA Special Papers. https://doi.org/10.1130/2006.2401(16)

Abelson M, Baer G, Shtivelman V, Wachs D, Raz E, Crouvi O, Kurzon I, Yechieli Y (2003) Collapse-sinkholes and radar interferometry reveal neotectonics concealed within the Dead Sea basin. Geophys Res Lett 30. https://doi.org/10.1029/2003gl017103

Abou Karaki N, Fiaschi S, Closson D (2016) Sustainable development and anthropogenic induced geomorphic hazards in subsiding areas. Earth Surf Processes Landforms 41:2282–2295. https://doi.org/10.1002/esp.4047

Al-Halbouni D, Holohan EP, Saberi L, Alrshdan H, Sawarieh A, Closson D, Walter TR, Dahm T (2017) Sinkholes, subsidence and subrosion on the eastern shore of the Dead Sea as revealed by a close-range photogrammetric survey. Geomorphology 285:305–324. https://doi.org/10.1016/j.geomorph.2017.02.006

Al-Halbouni D, Holohan EP, Taheri A, Watson RA, Polom U, Schöpfer MPJ, Emam S, Dahm T (2019) Distinct element geomechanical modelling of the formation of sinkhole clusters within large-scale karstic depressions. Solid Earth 10:1219–1241. https://doi.org/10.5194/se-10-1219-2019

Al-Halbouni D, Watson RA, Holohan EP, Meyer R, Polom U, Dos Santos FM, Comas X, Alrshdan H, Krawczyk CM, Dahm T (2021) Dynamics of hydrological and geomorphological processes in evaporite karst at the eastern Dead Sea—a multidisciplinary study. Hydrol Earth Syst Sci 25:3351–3395. https://doi.org/10.5194/hess-25-3351-2021

Arav R, Filin S, Avni Y (2020) Sinkhole swarms from initiation to stabilisation based on in situ high-resolution 3-D observations. Geomorphology 351:106916. https://doi.org/10.1016/j.geomorph.2019.106916

Avni Y, Lensky N, Dente E, Shviro M, Arav R, Gavrieli I, Yechieli Y, Abelson M, Lutzky H, Filin S, Haviv I, Baer G (2016) Self-accelerated development of salt karst during flash floods along the Dead Sea Coast, Israel. J Geophys Res Earth Surf 121:17–38. https://doi.org/10.1002/2015jf003738

Baer G, Schattner U, Wachs D, Sandwell D, Wdowinski S, Frydman S (2002) The lowest place on Earth is subsiding—An InSAR (interferometric synthetic aperture radar) perspective. GSA Bull 114:12–23. https://doi.org/10.1130/0016-7606(2002)114%3c0012:TLPOEI%3e2.0.CO;2

Baer G, Magen Y, Nof RN, Raz E, Lyakhovsky V, Shalev E (2018) InSAR measurements and viscoelastic modeling of sinkhole precursory subsidence: implications for sinkhole formation, early warning, and sediment properties. J Geophys Res Earth Surf 123:678–693. https://doi.org/10.1002/2017jf004594

Bates PD, Quinn N, Sampson C, Smith A, Wing O, Sosa J, Savage J, Olcese G, Neal J, Schumann G, Giustarini L, Coxon G, Porter JR, Amodeo MF, Chu Z, Lewis-Gruss S, Freeman NB, Houser T, Delgado M, Hamidi A, Bolliger I, McCusker K, Emanuel K, Ferreira CM, Khalid A, Haigh ID, Couasnon A, Kopp R, Hsiang S, Krajewski WF (2021) Combined modeling of US fluvial, pluvial, and coastal flood hazard under current and future climates. Water Resour Res 57. https://doi.org/10.1029/2020wr028673

Bayrak E, Yılmaz Ş, Softa M, Türker T, Bayrak Y (2015) Earthquake hazard analysis for East Anatolian Fault Zone, Turkey. Nat Hazards 76:1063–1077. https://doi.org/10.1007/s11069-014-1541-5

Beck B (2012) Soil Piping and Sinkhole Failures. In: White WB, Culver DC (eds) Encyclopedia of Caves, 2nd edn. Academic Press, Amsterdam, pp 718–723

Bernatek-Jakiel A, Gutiérrez F, Nadal-Romero E, Jakiel M (2019) Exploring the frequency-size relationships of pipe collapses in different morphoclimatic regions. Geomorphology 345:106845. https://doi.org/10.1016/j.geomorph.2019.106845

Bonachea J, Remondo J, de Terán JRD, González-Díez A, Cendrero A (2009) Landslide risk models for decision making. Risk Anal 29:1629–1643. https://doi.org/10.1111/j.1539-6924.2009.01283.x

Casas D, Chiocci F, Casalbore D, Ercilla G, de Urbina JO (2016) Magnitude-frequency distribution of submarine landslides in the Gioia Basin (southern Tyrrhenian Sea). Geo-Mar Lett 36:405–414. https://doi.org/10.1007/s00367-016-0458-2

Charrach J (2019) Investigations into the Holocene geology of the Dead Sea basin. Carbonates Evaporites 34:1415–1442. https://doi.org/10.1007/s13146-018-0454-x

Chiverrell RC, Sear DA, Warburton J, Macdonald N, Schillereff DN, Dearing JA, Croudace IW, Brown J, Bradley J (2019) Using lake sediment archives to improve understanding of flood magnitude and frequency: recent extreme flooding in northwest UK. Earth Surf Processes Landforms 44:2366–2376. https://doi.org/10.1002/esp.4650

Cloete G, Benito G, Grodek T, Porat N, Enzel Y (2018) Analyses of the magnitude and frequency of a 400-year flood record in the Fish River Basin, Namibia. Geomorphology 320:1–17. https://doi.org/10.1016/j.geomorph.2018.07.025

Closson D (2005) Structural control of sinkholes and subsidence hazards along the Jordanian Dead Sea coast. Environ Geol 47:290–301. https://doi.org/10.1007/s00254-004-1155-4

Closson D, Karaki NA (2009) Salt karst and tectonics: Sinkholes development along tension cracks between parallel strike-slip faults, Dead Sea, Jordan. Earth Surf Processes Landforms 34:1408–1421. https://doi.org/10.1002/esp.1829

Closson D, Pasquali P, Riccardi P, Milisavljevic N, Abou Karaki N (2013) The water deficit in the Middle East and the disappearance of the Dead Sea. In: De Boever M, Khlosi M, Delbecque N, De Pue J, Ryken N, Verdoodt A, Cornelis W, Gabriëls D (eds) Desertification and land degradation: processes and mitigation, UNESCO Chair of Eremology. Ghent University, Belgium, pp 16–24

Coianiz L, Bialik OM, Ben-Avraham Z, Lazar M (2019) Late Quaternary lacustrine deposits of the Dead Sea basin: high resolution sequence stratigraphy from downhole logging data. Quat Sci Rev 210:175–189. https://doi.org/10.1016/j.quascirev.2019.03.009

Coianiz L, Schattner U, Lang G, Ben-Avraham Z, Lazar M (2020) Between plate and salt tectonics—New stratigraphic constraints on the architecture and timing of the Dead Sea basin during the Late Quaternary. Basin Res 32:636–651. https://doi.org/10.1111/bre.12387

Cooper AH (2002) Environmental problems caused by gypsum karst and salt karst in Great Britain. Carbonates Evaporites 17:116–120. https://doi.org/10.1007/BF03176477

Coppersmith KJ, Youngs RR, Sprecher C (2009) Methodology and main results of seismic source characterization for the PEGASOS Project, Switzerland. Swiss J Geosci 102:91–105. https://doi.org/10.1007/s00015-009-1309-1

Corominas J, Mavrouli O, Ruiz-Carulla R (2018) Magnitude and frequency relations: are there geological constraints to the rockfall size? Landslides 15:829–845. https://doi.org/10.1007/s10346-017-0910-z

Corral Á, González Á (2019) Power law size distributions in geoscience revisited. Earth Space Sci. https://doi.org/10.1029/2018EA000479

Crozier MJ (2010) Deciphering the effect of climate change on landslide activity: a review. Geomorphology 124:260–267. https://doi.org/10.1016/j.geomorph.2010.04.009

Cruden DM, Fell R (2018) Quantitative risk assessment for slopes and landslides—The state of the art: IUGS Working Group on Landslides, Committee on Risk Assessment. Landslide risk assessment 3–12

Cruden DM, Hu XQ (1993) Exhaustion and steady state models for predicting landslide hazards in the Canadian Rocky Mountains. Geomorphology 8:279–285. https://doi.org/10.1016/0169-555X(93)90024-V

Dai FC, Lee CF (2001) Frequency–volume relation and prediction of rainfall-induced landslides. Eng Geol 59:253–266. https://doi.org/10.1016/S0013-7952(00)00077-6

De Waele J, Gutierrez F (2022) Karst Hydrogeology. Wiley, Geomorphology and Caves

Ezersky M, Frumkin A (2013) Fault—Dissolution front relations and the Dead Sea sinkhole problem. Geomorphology 201:35–44. https://doi.org/10.1016/j.geomorph.2013.06.002

Ezersky M, Frumkin A (2020) Identification of sinkhole origin using surface geophysical methods, Dead Sea. Israel Geomorphol 364:107225. https://doi.org/10.1016/j.geomorph.2020.107225

Ezersky M, Frumkin A (2021) Subaerial morphology affected by groundwater aggressiveness: Sinkhole susceptibility above karstified salt. Dead Sea Geomorphol 375:107525. https://doi.org/10.1016/j.geomorph.2020.107525

Ezersky M, Legchenko A, Camerlynck C, Al-Zoubi A (2009) Identification of sinkhole development mechanism based on a combined geophysical study in Nahal Hever South area (Dead Sea coast of Israel). Environ Geol 58:1123–1141. https://doi.org/10.1007/s00254-008-1591-7

Filin S, Baruch A, Avni Y, Marco S (2011) Sinkhole characterization in the Dead Sea area using airborne laser scanning. Nat Hazards 58:1135–1154. https://doi.org/10.1007/s11069-011-9718-7

Frumkin A, Raz E (2001) Collapse and subsidence associated with salt karstification along the Dead Sea. Carbonates Evaporites 16:117–130. https://doi.org/10.1007/BF03175830

Frumkin A, Ezersky M, Al-Zoubi A, Akkawi E, Abueladas A-R (2011) The Dead Sea sinkhole hazard: geophysical assessment of salt dissolution and collapse. Geomorphology 134:102–117. https://doi.org/10.1016/j.geomorph.2011.04.023

Galve JP, Gutiérrez F, Lucha P, Guerrero J, Bonachea J, Remondo J, Cendrero A (2009) Probabilistic sinkhole modelling for hazard assessment. Earth Surf Processes Landforms 34:437–452. https://doi.org/10.1002/esp.1753

Galve JP, Remondo J, Gutiérrez F (2011) Improving sinkhole hazard models incorporating magnitude–frequency relationships and nearest neighbor analysis. Geomorphology 134:157–170. https://doi.org/10.1016/j.geomorph.2011.05.020

Garfunkel Z, Ben-Avraham Z (1996) The structure of the Dead Sea basin. Tectonophysics 266:155–176. https://doi.org/10.1016/s0040-1951(96)00188-6

Gutenberg B, Richter CF (1954) Frequency and energy of earthquakes. Seismicity of the Earth and Associated Phenomena

Gutiérrez F, Lizaga I (2016) Sinkholes, collapse structures and large landslides in an active salt dome submerged by a reservoir: the unique case of the Ambal ridge in the Karun River, Zagros Mountains. Iran Geomorphol 254:88–103. https://doi.org/10.1016/j.geomorph.2015.11.020

Gutiérrez F, Parise M, De Waele J, Jourde H (2014) A review on natural and human-induced geohazards and impacts in karst. Earth-Sci Rev 138:61–88. https://doi.org/10.1016/j.earscirev.2014.08.002

Gutiérrez F (2016) Sinkhole hazards. In: Gutiérrez F (ed) Oxford Research Encyclopedia of Natural Hazard Science. Oxford University Press

Guzzetti F, Malamud BD, Turcotte DL, Reichenbach P (2002) Power-law correlations of landslide areas in central Italy. Earth Planet Sci Lett 195:169–183. https://doi.org/10.1016/S0012-821X(01)00589-1

Hounkpè J, Diekkrüger B, Afouda AA, Sintondji LOC (2019) Land use change increases flood hazard: a multi-modelling approach to assess change in flood characteristics driven by socio-economic land use change scenarios. Nat Hazards 98:1021–1050. https://doi.org/10.1007/s11069-018-3557-8

Hufschmidt G, Crozier MJ (2008) Evolution of natural risk: analysing changing landslide hazard in Wellington, Aotearoa/New Zealand. Nat Hazards 45:255–276. https://doi.org/10.1007/s11069-007-9158-6

Kundzewicz ZW, Pińskwar I, Brakenridge GR (2017) Changes in river flood hazard in Europe: a review. Hydrol Res 49:294–302. https://doi.org/10.2166/nh.2017.016

Machado MJ, Botero BA, López J, Francés F, Díez-Herrero A, Benito G (2015) Flood frequency analysis of historical flood data under stationary and non-stationary modelling. Hydrol Earth Syst Sci 19:2561–2576. https://doi.org/10.5194/hess-19-2561-2015

Malamud BD, Turcotte DL, Guzzetti F, Reichenbach P (2004) Landslide inventories and their statistical properties. Earth Surf Processes Landforms 29:687–711. https://doi.org/10.1002/esp.1064

Malamud BD (2004) Tails of natural hazards. PHYSICS WORLD

Mor O, Burg A (2000) Geological Map of Israel, Sheet 12-III, Mizpe Shalem, 1: 50,000. Geological Survey of Israel, Jerusalem

Neugebauer I, Brauer A, Schwab MJ, Waldmann ND, Enzel Y, Kitagawa H, Torfstein A, Frank U, Dulski P, Agnon A, Ariztegui D, Ben-Avraham Z, Goldstein SL, Stein M, Party DS (2014) Lithology of the long sediment record recovered by the ICDP Dead Sea deep drilling project (DSDDP). Quat Sci Rev 102:149–165. https://doi.org/10.1016/j.quascirev.2014.08.013

Nof RN, Abelson M, Raz E, Magen Y, Atzori S, Salvi S, Baer G (2019) SAR interferometry for sinkhole early warning and susceptibility assessment along the Dead Sea. Israel Remote Sens 11:89. https://doi.org/10.3390/rs11010089

Pacheco JF, Scholz CH, Sykes LR (1992) Changes in frequency–size relationship from small to large earthquakes. Nature 355:71–73. https://doi.org/10.1038/355071a0

Parise M (2019) Chapter 110 - Sinkholes. In: White WB, Culver DC, Pipan T (eds) Encyclopedia of Caves (Third Edition). Academic Press, pp 934–942

Parise M, Closson D, Gutiérrez F, Stevanović Z (2015) Anticipating and managing engineering problems in the complex karst environment. Environ Earth Sci 74:7823–7835. https://doi.org/10.1007/s12665-015-4647-5

Pebesma E (2018) Simple features for R: Standardized support for spatial vector data. R J 10:439. https://doi.org/10.32614/rj-2018-009

R Core Team (2022) R: A language and environment for statistical computing. R Foundation for Statistical Computing, Vienna, Austria

Remondo J, Bonachea J, Cendrero A (2005) A statistical approach to landslide risk modelling at basin scale: from landslide susceptibility to quantitative risk assessment. Landslides 2:321–328. https://doi.org/10.1007/s10346-005-0016-x

Salameh E, Alraggad M, Amaireh M (2019) Degradation processes along the new northeastern shores of the Dead Sea. Environ Earth Sci 78:164. https://doi.org/10.1007/s12665-019-8155-x

Sevil J, Gutiérrez F (2023) Morphometry and evolution of sinkholes on the western shore of the Dead Sea. Implicat Suscep Assess Geomorphol 434:108732. https://doi.org/10.1016/j.geomorph.2023.108732

Shalev E, Lyakhovsky V, Yechieli Y (2006) Salt dissolution and sinkhole formation along the Dead Sea shore. J Geophys Res. https://doi.org/10.1029/2005JB004038

Song K-I, Cho G-C, Chang S-B (2012) Identification, remediation, and analysis of karst sinkholes in the longest railroad tunnel in South Korea. Eng Geol 135–136:92–105. https://doi.org/10.1016/j.enggeo.2012.02.018

Taheri K, Gutiérrez F, Mohseni H, Raeisi E, Taheri M (2015) Sinkhole susceptibility mapping using the analytical hierarchy process (AHP) and magnitude–frequency relationships: a case study in Hamadan province, Iran. Geomorphology 234:64–79. https://doi.org/10.1016/j.geomorph.2015.01.005

Tolmachev V, Leonenko M (2011) Experience in collapse risk assessment of building on covered karst landscapes in Russia. In: van Beynen PE (ed) Karst Management. Springer, Netherlands, pp 75–102

van Westen CJ, van Asch TWJ, Soeters R (2006) Landslide hazard and risk zonation—why is it still so difficult? Bull Eng Geol Environ 65:167–184. https://doi.org/10.1007/s10064-005-0023-0

Vey S, Al-Halbouni D, Haghighi MH, Alshawaf F, Vüllers J, Güntner A, Dick G, Ramatschi M, Teatini P, Wickert J, Weber M (2021) Delayed subsidence of the Dead Sea shore due to hydro-meteorological changes. Sci Rep 11:13518. https://doi.org/10.1038/s41598-021-91949-y

Waltham AC, Bell FG, Culshaw MG (2005) Sinkholes and Subsidence. Springer, Berlin Heidelberg

Watson RA, Holohan EP, Al-Halbouni D, Saberi L, Sawarieh A, Closson D, Alrshdan H, Abou Karaki N, Siebert C, Walter TR, Dahm T (2019) Sinkholes and uvalas in evaporite karst: spatio-temporal development with links to base-level fall on the eastern shore of the Dead Sea. Solid Earth 10:1451–1468. https://doi.org/10.5194/se-10-1451-2019

Wickham H, Averick M, Bryan J, Chang W, McGowan L, François R, Grolemund G, Hayes A, Henry L, Hester J, Kuhn M, Pedersen T, Miller E, Bache S, Müller K, Ooms J, Robinson D, Seidel D, Spinu V, Takahashi K, Vaughan D, Wilke C, Woo K, Yutani H (2019) Welcome to the tidyverse. J Open Source Softw 4:1686. https://doi.org/10.21105/joss.01686

Yechieli Y, Abelson M, Bein A, Crouvi O, Shtivelman V (2006) Sinkhole "swarms" along the Dead Sea coast: Reflection of disturbance of lake and adjacent groundwater systems. GSA Bull 118:1075–1087. https://doi.org/10.1130/B25880.1

Yechieli Y, Abelson M, Baer G (2016) Sinkhole formation and subsidence along the Dead Sea coast, Israel. Hydrogeol J 24:601–612. https://doi.org/10.1007/s10040-015-1338-y

Yizhaq H, Ish-Shalom C, Raz E, Ashkenazy Y (2017) Scale-free distribution of Dead Sea sinkholes: observations and modeling. Geophys Res Lett 44:4944–4952. https://doi.org/10.1002/2017gl073655